American Mineralogist, Volume 89, pages 633–639, 2004

Isothermal equation of state and compressional behavior of tetragonal edingtonite

GIACOMO DIEGO GATTA,[1,*] TIZIANA BOFFA BALLARAN,[1] PAOLA COMODI,[2] AND PIER FRANCESCO ZANAZZI[2]

[1]Bayerisches Geoinstitut, Universitaet Bayreuth, Universitaet Strasse 30, D-95447 Bayreuth, Germany
[2]Dipartimento di Scienze della Terra, Università di Perugia, Piazza Università, I-06100 Perugia, Italy

ABSTRACT

The high-pressure (H*P*) structural evolution of a natural tetragonal edingtonite from Ice River, Canada, was investigated up to 5.1 GPa using in situ single-crystal X-ray diffraction and a diamond-anvil cell. The isothermal equation of state was determined. The values of V_0, K_{T0}, and K' refined with a third-order Birch-Murnaghan equation of state (BM-EoS) are V_0 = 601.6(3) Å^3, K_{T0} = 59(2) GPa, and K' = 3.4(8). Under high-pressure conditions the main deformation mechanisms can be described by rotation/kinking of "rigid units," represented by the 4 = 1 secondary building unit (SBU), due to the tetrahedra tilting. The angle between the SBUs (ϕ) increased from 17.15(8)° at 0.0001 GPa to 20.03(9)° at 4.61 GPa.

The bulk structural compression results from the combination of the "soft" behavior of the not fully occupied channels [K_{T0} = 19(1) GPa for [100]-channels; K_{T0} = 21(1) GPa for [110]-channels] and of the rigid behavior of the tetrahedral framework.

The extra-framework cations do not increase in coordination number within the pressure range investigated. The barium occupancy factors for the Ba1 and Ba2 sites change with increasing pressure. For $P > 2.3$ GPa the Ba2 site is completely empty, and only the position Ba1 is occupied.

INTRODUCTION

According to Gottardi and Galli (1985) and Armbruster and Gunter (2001), edingtonite belongs to the "fibrous zeolites" group, with ideal chemical composition $Ba_2Al_4Si_6O_{20}\cdot 8H_2O$. The structure of edingtonite was determined by Taylor and Jackson (1933) in the $P\bar{4}2_1m$ space group. Galli (1976) and Kvick and Smith (1983) refined the crystal structure in $P\,2_12_12$. The difference between tetragonal and orthorhombic edingtonite is due to (Si,Al)-disorder/order in the tetrahedra which reduces the lattice symmetry from $P\bar{4}2_1m$ to $P\,2_12_12$. Mazzi et al. (1984) reinvestigated the crystal structure of tetragonal edingtonite, giving new details on the extra-framework content.

The framework of this fibrous zeolite consists of tetrahedral chains, with topological symmetry $P\bar{4}2_1m$, running along [001] (Fig. 1). The basic building block for these chains is the "4 = 1 secondary building unit (SBU)" (Baerlocher et al. 2001), shown in Figure 1. The framework encloses two systems of channels: 8-ring channels along [001] and 8-ring channels along [110]. These channels contain the extra-framework cations and water molecules.

In edingtonite there is only one extra-framework cation site, preferentially occupied by Ba, and two independent water molecule sites. Six framework O atoms and four water molecules make up the Ba coordination polyhedron. According to Mazzi et al. (1984), in tetragonal edingtonite the Ba site is split into two sites ~0.46 Å apart. Most of Ba cations (up to 90%) are at the Ba1 site and a minor amount (<10%) at the Ba2 site; the sum of the occupancy factors of the two sites is lower than 100%.

The structural thermal stability of orthorhombic edingtonite was investigated by Belitsky et al. (1986) and Ståhl and Hanson (1998). The study of the structure and dynamics of water at low temperature (100 K) by neutron diffraction and NMR spectroscopy showed a phase transition to *P*2, at ~210 K, due to the changes in the hydrogen positions (Belitsky et al. 1986). On the other hand, the study of edingtonite dehydration using X-ray synchrotron powder diffraction showed a continuous loss of water up to 660 K. Above 660 K, the crystal structure is rapidly destroyed (Ståhl and Hanson 1998). Other information on the thermal stability and thermodynamic parameters of edingtonite can be found in van Reeuwijk (1972, 1974), Mazzi et al. (1984), Goryainov and Belitsky (1986), and Belitsky et al. (1992).

Only two studies of the high-pressure (H*P*) structural evolution of fibrous zeolites, scolecite and natrolite, are reported in the literature (Comodi et al. 2002; Lee et al. 2002). Other studies of fibrous zeolites at high pressure reported only the cell volume variation but not experimental structural data (Belitsky et al. 1992; Goryainov and Smirnov 2001; Ballone et al. 2002).

The aim of our study is to investigate the structural evolution of tetragonal edingtonite under pressure using in situ X-ray single-crystal diffraction. This information will then be compared with the H*P* behavior of scolecite and natrolite in order to obtain a general mechanism of deformation for fibrous zeolites at H*P*. Moreover, a comparison between the high-pressure and high-temperature transformations of edingtonite will be carried out.

EXPERIMENTAL METHODS

The edingtonite specimen used is from Ice River, Canada. E. Galli and E. Passaglia from the University of Modena kindly provided the crystals and chemical data. Details on the microprobe and TG analysis are reported in Mazzi et al. (1984). The unit-cell content is $(Ba_{1.82}Sr_{0.01}K_{0.11}Na_{0.03})(Al_{3.90}Si_{6.13})O_{20}\cdot 7.30H_2O$.

Single-crystal X-ray diffraction data was obtained with an XCALIBUR Oxford

* E-mail: diego.gatta@uni-bayreuth.de

Instruments diffractometer equipped with a CCD, using graphite-monochromatized Mo*K*α (λ = 0.7107 Å) radiation, and operated at 50 kV and 30 mA. To maximize the reciprocal space coverage a combination of ω and ϕ scans was used, with a step size of 0.5° and a time of 20 s/frame. The distance between the crystal and the detector was 60.4 mm. 10809 reflections in the range $3 < \theta < 35°$ were collected, of which 1371 were unique, giving metrically tetragonal cell parameters $a = b = 9.5909(10)$ Å, $c = 6.5339(10)$ Å, $V = 601.02(30)$ Å^3. After Lorentz, polarization, and empirical absorption corrections using the SADABS package (Sheldrick 1996), the discrepancy factor among symmetrically related reflections was $R_{int} = 0.038$. The refinement was carried out with isotropic displacement parameters in space group $P\bar{4}2_1m$ using the SHELXL-97 package (Sheldrick 1997) and initial atomic coordinates from Mazzi et al. (1984). Since the hydrogen atoms cannot be observed in the H*P* refinements, they were not included in the room-pressure refinement. The final least-square cycles were conducted with anisotropic thermal parameters and with Ba1, Ba2, OW1, and OW2 occupancy factors fixed at values obtained from the isotropic refinement. This strategy was applied because our previous refinements of tetragonal edingtonite showed a systematic strong correlation between barium/water occupancy factors and anisotropic thermal parameters.

The final agreement index (R_1) was 0.019 for 57 refined parameters and 604 unique reflections with $F_o > 4\sigma(F_o)$. Details of crystal and refinement data are reported in Tables 1–3. The neutral atomic scattering factor values from the *International Tables for X-ray Crystallography* (Ibers and Hamilton 1974) were used. For the extra-framework Ba1 and Ba2 sites the scattering curve of barium alone was used, varying the site occupancy factors. For the tetrahedral sites (T1 and T2) the scattering curve of silicon was used. A structure refinement performed using the ionic scattering curves did not provide significantly different results.

A BGI diamond anvil cell (DAC) designed by Allan et al. (1996) was used for the high-pressure study. Steel T301 foil, 250 μm thick with a 350 μm hole, was used as gasket.

Glycerol was used as a non-penetrating pressure-transmitting medium because its large-sized molecules do not enter into the zeolite framework channels. This medium has been successfully used in previous studies of microporous materials up to 4–5 GPa (Hazen and Finger 1984; Comodi et al. 2001, 2003). Ruby chips (Mao et al. 1986) and a single crystal of quartz as internal standard (Angel et al. 1997) were used for pressure calibration.

The lattice parameters were determined at pressures ranging between 0.0001 and 5.08 GPa (Table 2) at the Bayerisches Geoinstitut with a Huber four-circle diffractometer (Mo*K*α) using eight-position centering of 25 Bragg reflections (King and Finger 1979; Angel et al. 2000). Centering procedure and least-square fitting of the unit-cell parameters were performed with the SINGLE software (Angel et al. 2000).

Intensity data were collected with a Nonius CAD4 diffractometer (Mo*K*α) at 0.0001 GPa (crystal in DAC without pressure medium), 2.28(1), and 4.61(2) GPa up to θ = 30°. Scan type, scan width, and scan speed are reported in Table 1.

TABLE 1. Details of data collection and refinements of edingtonite at different pressures

Pressure (GPa)	0.0001	0.0001*	2.28(1)	4.61(2)
Crystal size (μm)	140 × 180 × 90	200 × 100 × 60	200 × 100 × 60	200 × 100 × 60
Radiation	Mo*K*α	Mo*K*α	Mo*K*α	Mo*K*α
Detector type	CCD	Point det.	Point det.	Point det.
θ range (°)	3–35	1–30	1–30	1–30
Scan type	ω/ϕ	ω	ω	ω
Scan speed (°/min)	–	2.06	2.06	3.29
Scan width (°)	0.5°/frame	0.7	0.8	1.5
CCD frame processed	1402	–	–	–
Exposure time/frame (s/frame)	20	–	–	–
Space group	$P\bar{4}2_1m$	$P\bar{4}2_1m$	$P\bar{4}2_1m$	$P\bar{4}2_1m$
Reflections measured	10809	865	836	333
Unique refl. (total)	1371	446	574	262
Unique refl. with $F_o > 4\sigma(F_o)$	604	277	364	193
Parameters refined	57	32	30	27
R_{int}	0.038	0.058	0.052	0.050
R_1 (F)	0.019	0.057	0.053	0.054
GooF	0.862	1.142	1.133	1.126

* Data collected under room conditions with the crystal in the DAC without the pressure medium.

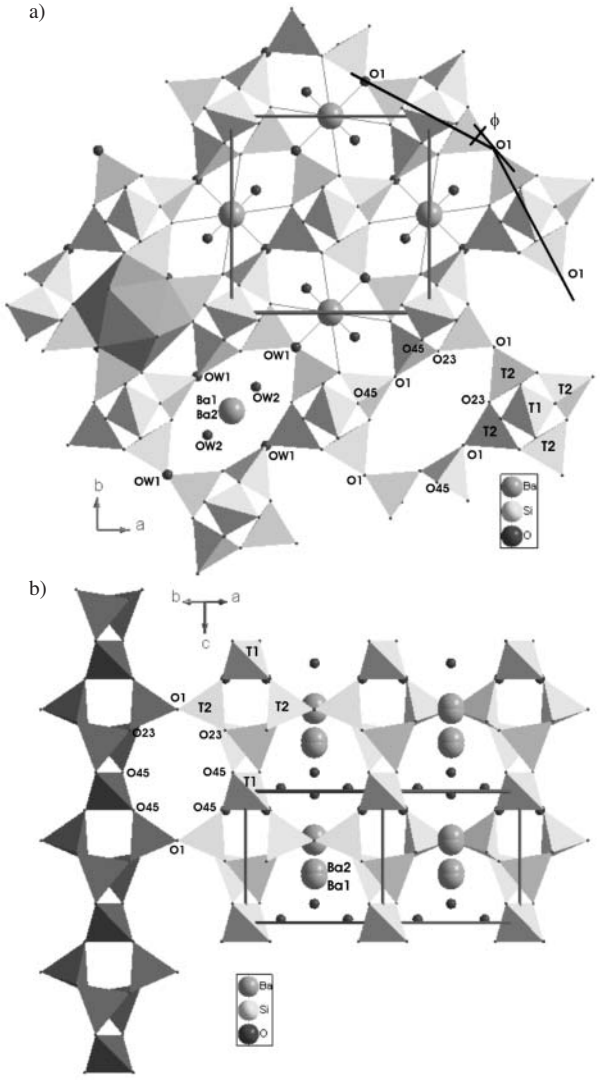

FIGURE 1. (**a**) Projection of the crystal structure of edingtonite viewed down [001], and (**b**) viewed down [110], showing the SBU chains along [001] (dark gray). The two channel systems and the extra-framework population are shown. The large spheres represent cation sites, whereas the small spheres represent the O atom of the water molecules. One Ba coordination polyhedron is shown.

TABLE 2. Lattice parameters of tetragonal edingtonite at different pressures

P (GPa)	*a* (Å)	*c* (Å)	*V* (Å)^3
0.0001	9.5909(14)	6.5339(19)	601.03(24)
0.689(8)	9.5602(9)	6.5117(13)	595.15(17)
1.080(8)	9.5383(9)	6.5021(13)	591.56(17)
1.312(8)	9.5277(33)	6.4988(44)	589.95(56)
1.539(8)	9.5117(9)	6.4904(12)	587.21(15)
1.998(8)	9.4838(9)	6.4801(13)	582.85(16)
2.28(1)	9.4669(24)	6.4765(33)	580.41(41)
2.70(2)	9.4435(9)	6.4651(14)	576.56(17)
3.05(1)	9.4239(7)	6.4576(10)	573.51(12)
3.45(2)	9.4019(7)	6.4489(10)	570.07(12)
4.61(2)	9.3466(6)	6.42705(9)	561.46(10)
5.08(3)	9.3279(10)	6.4169(14)	558.34(16)
1.564(8)*	9.5120(9)	6.4906(12)	587.26(15)
0.908(8)*	9.5482(11)	6.5076(17)	593.28(19)

* Data collected during decompression.

TABLE 3. Refined positional and displacement parameters (Å²) for edingtonite at different pressures

Site	x	y	z	Site occupancy	U_{iso}/U_{eq}
Ba1	0.5	0.0	0.64292(22)	0.79(1)	0.01583(27)
	0.5	0.0	0.6448(11)	0.76(3)	0.0193(11)
	0.5	0.0	0.64407(91)	0.84(4)	0.0156(10)
	0.5	0.0	0.64515(30)	0.89(2)	0.01287(63)
Ba2	0.5	0.0	0.5938(11)	0.15(1)	0.0138(12)
	0.5	0.0	0.5938(66)	0.15(3)	0.0269(49)
	0.5	0.0	0.599(31)	0.04(4)	0.035(16)
	–	–	–	0.0	–
T1	0.0	0.0	0.0	1.0	0.00933(24)
	0.0	0.0	0.0	1.0	0.0148(12)
	0.0	0.0	0.0	1.0	0.0185(11)
	0.0	0.0	0.0	1.0	0.0170(19)
T2	–0.17347(7)	0.09318(8)	0.38107(14)	1.0	0.00934(16)
	–0.17337(36)	0.09321(38)	0.38132(49)	1.0	0.01698(94)
	–0.17650(32)	0.08882(32)	0.38125(42)	1.0	0.01860(85)
	–0.17921(57)	0.08614(59)	0.38026(55)	1.0	0.0139(13)
O1	0.17297(22)	0.32703(22)	0.62436(62)	1.0	0.01337(53)
	0.17285(98)	0.32715(98)	0.6195(18)	1.0	0.0209(25)
	0.16745(79)	0.33255(95)	0.6277(15)	1.0	0.0179(20)
	0.1588(5)	0.3411(14)	0.6303(22)	1.0	0.0153(35)
O23	–0.04481(24)	0.19643(25)	0.46501(43)	1.0	0.01664(46)
	–0.04456(88)	0.1945(11)	0.4665(13)	1.0	0.0227(22)
	–0.05014(81)	0.19435(9)	0.4589(11)	1.0	0.0229(18)
	–0.0508(14)	0.1909(19)	0.4544(15)	1.0	0.0236(32)
O45	–0.13667(22)	0.03769(23)	0.14424(47)	1.0	0.01659(41)
	–0.1364(10)	0.03823(89)	0.1456(13)	1.0	0.0219(20)
	–0.14302(80)	0.03088(75)	0.1435(11)	1.0	0.0242(17)
	–0.1480(15)	0.0230(15)	0.1438(14)	1.0	0.0203(25)
OW1	0.17659(46)	0.32341(46)	0.1461(11)	0.79(2)	0.0310(11)
	0.1786(17)	0.3213(17)	0.1405(33)	0.74(6)	0.0376(72)
	0.1793(10)	0.3206(10)	0.1552(19)	0.74	0.0160(26)
	0.1851(18)	0.3148(18)	0.1613(30)	0.74	0.0106(42)
OW2	0.37786(55)	0.12214(55)	–0.0251(14)	0.98(4)	0.0581(19)
	0.3740(19)	0.1259(19)	–0.0192(33)	0.92(7)	0.066(10)
	0.3774(15)	0.1225(15)	–0.0136(25)	0.92	0.0499(43)
	0.3757(23)	0.1243(23)	–0.0170(30)	0.92	0.0446(65)

Notes: For each atom, values from top to bottom correspond to the refinement at 0.0001 GPa in air, 0.0001 GPa in the DAC, 2.28(1) and 4.61(2) GPa respectively. For H*P* refinements the isotropic thermal parameters, U_{iso}, are reported, whereas for the room condition refinements U_{eq} is shown.

Integrated intensity data were obtained using the WININTEGRSTP3.4 program (Angel 2003a,b). A correction for Lorentz and polarization effects was applied. Finally, diffraction data were corrected for crystal and pressure-cell absorption with the ABSORB5.2 program (Burnham 1966; Angel 2002).

The H*P* structures were refined with isotropic atomic displacement parameters and the water site occupancies (OW1, OW2) were fixed to the values obtained under room conditions (with the crystal in the DAC). Least-squares refinements were performed with the SHELX-97 software (Sheldrick 1997).

Details of the refinements are listed in Table 1–3. Observed and calculated structure factors can be obtained from the authors upon request (or through the Editorial Office).

RESULTS

Room conditions

The crystal structure of edingtonite was refined at room pressure in air and in a DAC with starting coordinates from Mazzi et al. (1984). The refined coordinates of the framework and extra-framework atoms (Table 3) are very close to those found for edingtonite from Ice River (Canada) and for edingtonite from Old Kilpatrick (Scotland) by Mazzi et al. (1984). Special care was devoted to the location of the split Ba site (Ba1, Ba2) and water molecules (OW1, OW2).

We confirmed that in tetragonal edingtonite the Ba^{2+} site is split into two sites, in this case ~0.34 Å apart. Most of Ba cations occupy the Ba1 site (~76–80%) and a minor amount (~15%) the Ba2 site (Table 3); the sum of the occupancy factors of the two sites is lower than 100%. The occupancies of the water sites, 79% for OW1 and 98% for OW2 with the crystal in air, 74% for OW1 and 92% for OW2 with the crystal in the DAC (Table 3), are lower than the values observed by Mazzi et al. (1984).

The determination of Al-content in the tetrahedra was carried out using the geometrical considerations proposed by Alberti and Gottardi (1988). The result, from the refinement with the crystal in the DAC, is: T1(Al) = 39.98%, T2(Al) = 39.26%, with a total Al-content equal to 3.92 atoms per formula unit (apfu). This result is in good agreement with chemical data from the analysis and in complete accordance with the charge balance due to the Ba^{2+} content. Applying the method of Jones (1968), we obtain: T1(Al) = 35.51%, T2(Al) = 39.36%, with a total Al-content equal to 3.85 apfu. The Si/Al-disorder in the tetrahedra demonstrates the effective general tetragonal symmetry of this specimen. T1-O and T2-O bond distances are reported in Table 4.

Compressibility

The variation of the lattice parameters of tetragonal edingtonite with pressure (Table 2), normalized to the value corresponding to room conditions, is shown in Figure 2. A volume finite strain-stress plot (*fe-Fe* plot; Angel 2000) is reported in Figure 3a and a weighted linear regression through the data points is shown.

Unit-cell volume data were fitted with a third order Birch-Murnaghan Equation of State (BM-EoS) (Birch 1947), with the EOS-FIT5.2 program (Angel 2001). Using the data weighted by the uncertainties in *P-V*, the results are: V_0 = 601.6(3) Å³, K_{T0} = 59(2) GPa, and K' = 3.4(8). The confidence ellipse (Fig. 4), calculated starting from the variance-covariance matrix of K_{T0} and K' obtained from the least-squares procedure, shows a strongly negative correlation. The individual values for K_{T0} and K' are 59(3) and 3.4(12), respectively.

To quantify the effect of the uncertainty in V_0 on the compression parameters (K_{T0}, K', *fe*, *Fe*), a second set of finite strain-stress data (Fig. 3b) has been determined using the V_0 value calculated from the third-order BM-EoS of all data but without the observed V_0 value. It is clear from a comparison of these two plots (Figs. 3a and b) that the observed V_0 has a strong effect on the data of the *fe-Fe* plot at low pressure. The BM-EoS parameters obtained excluding the observed V_0 value are: V_0 = 603.0(4) Å³, K_{T0} = 53(2) GPa, and K' = 5.5(8), which are in good agreement with the values calculated from the *fe-Fe* plot (Fig. 3b). The differences between the two set of EoS parameters show the relevant influence of the uncertainty in V_0 on the compression parameters when, as in this case, $\sigma_{V0} > 10^{-4}\ V_0$ (Angel 2000).

The evolution of the lattice constants with pressure shows an anisotropic compression pattern (Fig. 2). The axial bulk moduli were calculated with a third-order "linearized" BM-EoS (Angel 2000) using all data. The EoS parameters are: $K_{T0\mathbf{a}}$ = 53(3) and $K'_{\mathbf{a}}$ = 2(1) for the **a** axis and $K_{T0\mathbf{c}}$ = 73(4) and $K'_{\mathbf{c}}$ = 10(2) for the **c** axis ($K_{T0\mathbf{a}} : K_{T0\mathbf{b}} : K_{T0\mathbf{c}}$ = 1 : 1 : 1.4). To analyze the role of the uncertainty in a_0 and c_0, the linearized BM-EoS were also fitted without the room pressure a_0 and c_0 values. In this case the EoS parameters are: $K_{T0\mathbf{a}}$ = 45(2) and $K'_{\mathbf{a}}$ = 4.9(8), $K_{T0\mathbf{c}}$ = 80(6) and $K'_{\mathbf{c}}$ = 7(3) respectively ($K_{T0a} : K_{T0b} : K_{T0c}$ = 1 : 1 : 1.8), showing a slightly higher anisotropy. No phase transition was observed up to 5.08(3) GPa. Significant peak broadening was observed

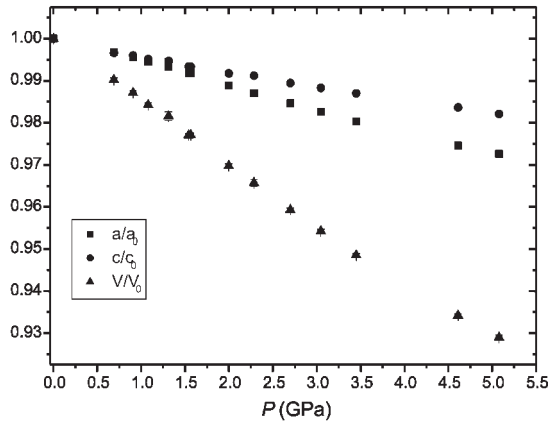

FIGURE 2. Variation as a function of *P* of the unit-cell parameters normalized with respect to the room pressure value. The e.s.d. values are smaller than the size of the symbols.

TABLE 4. Interatomic distances (Å) as a function of pressure

P (GPa)	0.0001	0.0001*	2.28(1)	4.61(2)
Ba1-O1 (×2)	2.9247(35)	2.912(13)	2.850(11)	2.747(17)
Ba1-O23 (×4)	3.0264(24)	3.049(10)	3.007(9)	2.997(17)
Ba1-OW1 (×2)	2.7636(58)	2.799(23)	2.730(13)	2.745(22)
Ba1-OW2 (×2)	2.7292(71)	2.782(23)	2.758(18)	2.722(24)
Ba2-O1 (×2)	2.7453(49)	2.727(25)	2.68(11)	–
Ba2-O23 (×4)	2.9681(26)	2.987(12)	2.957(27)	–
Ba2-OW1 (×2)	2.9367(72)	2.980(33)	2.88(11)	–
Ba2-OW2 (×2)	2.9904(95)	3.052(42)	2.99(16)	–
T1-O45 (×4)	1.6544(24)	1.6587(9)	1.668(7)	1.678(13)
T2-O1	1.6601(12)	1.661(5)	1.655(4)	1.660(8)
T2-O23	1.6767(27)	1.666(9)	1.682(8)	1.667(13)
T2-O23′	1.6746(25)	1.667(10)	1.638(8)	1.620(16)
T2-O45	1.6741(31)	1.666(9)	1.665(7)	1.656(10)
<T2-O>	1.6714	1.665	1.660	1.651

* Data collected under room conditions with the crystal in the DAC without the pressure medium.

at *P* higher than 4 GPa. At 5.5 GPa the large full-width-at-half-maximum (FWHM) interfered with the centering and the determination of the lattice parameters. Similar behavior was observed for quartz; the large FWHM of the peaks induced an inaccurate lattice determination for $P > 4$ GPa, giving a higher uncertainty for the *P* values obtained from the quartz-EoS (Table 2). This effect, observed for edingtonite and quartz, is clearly due to the pressure medium behavior, which is not completely hydrostatic up to 5 GPa.

The structural modifications induced within the pressure range investigated are completely reversible: the diffraction data acquired during decompression showed a complete restoration of the lattice constants (Fig. 2, Table 2).

In order to compare the high-pressure behavior of edingtonite with the other fibrous zeolites reported in literature, whose *K*' values were always fixed to 4, cell volume data were fitted with a second-order BM-EoS. Using data weighted by the uncertainties in *P-V*, we obtained: $V_0 = 601.8(2)$ Å^3 and $K_{T0} = 57.9(6)$ GPa, with $K' = 4$ (fixed); or if we exclude the observed V_0 value from the data, $V_0 = 602.3(2)$ Å^3, $K_{T0} = 56.9(4)$ GPa, and $K' = 4$ (fixed). The bulk modulus of edingtonite, using a non-penetrating pressure medium, appears slightly higher than the bulk moduli of other fibrous zeolites, such as scolecite [$K_{T0} = 54.6(7)$ GPa, $K' = 4$, Comodi et al. 2002] and natrolite [$K_{T0} = 53(1)$ GPa, $K' = 4$,

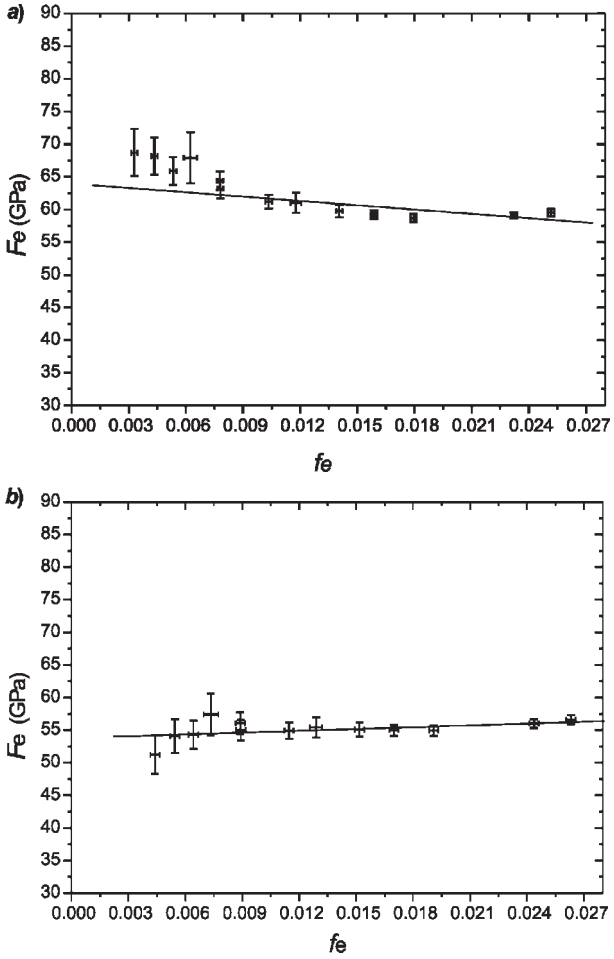

FIGURE 3. Plot of the volume finite strain $f_e = [(V_0/V)^{2/3} - 1]/2$ vs. the "normalized stress," defined as $F_e = P / [3f_e(1 + 2f_e)^{5/2}]$, for tetragonal edingtonite in glycerol. (**a**) *fe-Fe* plot calculated using the observed V_0 value and (**b**) *fe-Fe* plot calculated using the V_0 value obtained from the third-order BM-EoS (see text). The e.s.d. were calculated according to Heinz and Jeanloz (1984).

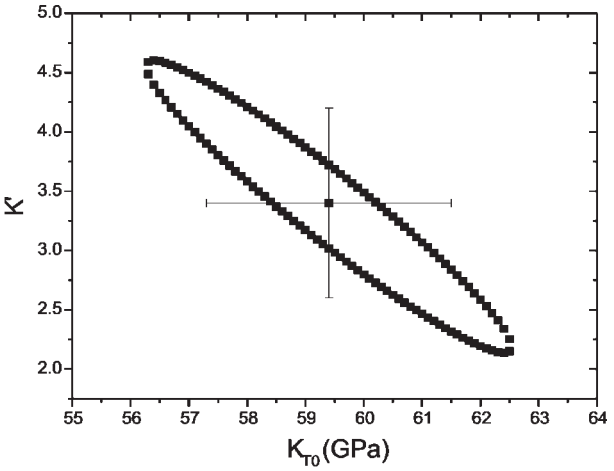

FIGURE 4. Confidence ellipse (at the 68.3% level) in K_{T0} and *K*' for the fit of third order BM-EoS to the edingtonite *P-V* data. Error bars are ±1 e.s.d.

before the phase transition at 1.5–2.0 GPa due to superhydration effects induced by the pressure medium, Lee et al. 2002].

Structural evolution with pressure: framework and extra-framework behavior

Structural refinements carried out at 0.0001, 2.28(1), and 4.61(2) GPa allowed us to understand the H*P* structural behavior of this zeolite. The structural deformations occurring with increasing pressure are compared with the crystal structure obtained at room conditions with the crystal in the DAC.

Increasing pressure does not induce relevant variations in the tetrahedral bond distances (Table 4) within the pressure range investigated. As expected for open framework structures, the main deformation occurs in the polyhedral tilting that produces inter-tetrahedral angle variations (Hazen and Finger 1979; Gatta et al. 2003). One "rigid unit," made up of a small group of tetrahedra and represented by the 4 = 1 SBU, was identified. The SBU volume, calculated considering the SBU as a distorted polyhedron with six vertices formed by the centers of the six nearest tetrahedra, changes from 15.52(3) Å^3 at ambient pressure, to 14.78(5) Å^3 at 4.61(2) GPa. Thus the SBU bulk modulus, calculated from a linear regression, is 97(8) GPa. As also observed in a previous study of scolecite (Comodi et al. 2002), the volume variation of the 4 = 1 SBU itself is due to tetrahedral tilting: the T1-O45-T2 angle changes from 140.18(8) to 134.34(10)°, and the distance between T2-T2 from 3.776(5) to 3.715(6) Å, in response to an applied pressure of 4.61(2) GPa (Table 5). The most relevant structural variations are produced by cooperative rotation ("antiroration") of the SBU along [001] (Fig. 5). As a consequence, the obtuse angle of the [001]-channel, O45-O1-O45°, increases from 108.74(10)°, at 0.0001 GPa, to 110.97(12)° at 4.61(2) GPa; on the contrary the acute angle, O23-O1-O23°, decreases from 79.21(9)°, at 0.0001 GPa, to 75.75(9)° at 4.61(2) GPa (Table 5). The angle between the [001]-chains, here defined as $\phi° = [180°-(O1-O1-O1)°]/2$ (Fig. 1), increases from 17.15(8)° at ambient conditions to 20.03(9)° at 4.61(2) GPa (Table 5). To compare the chain rotation effect of edingtonite under pressure with that of other fibrous zeolites, the ψ angle value, as defined by Alberti and Vezzalini (1981) and Baur et al. (1990), is reported in Table 5.

The channel ellipticity was modified as a consequence of the applied pressure. The ratio between the smaller "free diameter" (Baerlocher et al. 2001) and the larger one, $\varepsilon_{[001]}$ = O1-O1(short)/O1-O1(long) for the 8-ring channel along [001] and $\varepsilon_{[110]}$ = O45-O45(long)/O1-O1 for the 8-ring channel along [110] (Fig. 1), was calculated. $\varepsilon_{[001]}$ changes from 0.32 (P = 0.0001 GPa) to 0.24 (P = 4.61(2) GPa), whereas $\varepsilon_{[110]}$ changes from 0.72 (P = 0.0001 GPa) to 0.61 [P = 4.61(2) GPa] (Table 5). In other words, the ellipticities of the [001] and of the [110]-channels increase with pressure by about 25% and 15%, respectively. An increase of the pore ellipticity with pressure for fibrous zeolites was previously reported by Lee et al. (2000) for natrolite and by Comodi et al. (2002) for scolecite.

The antirotation mechanism produces compression on both the channel systems: the [001]- and [110]-channel bulk moduli,

TABLE 5. Relevant structural parameters for edingtonite at different pressures

P (GPa)	0.0001*	2.28(1)	4.61(2)	K_{T0} (GPa)
V SBU (Å^3)	15.52(3)	15.12(4)	14.78(5)	97(8)
T1-T1 (Å)	6.534(6)	6.477(7)	6.427(6)	
T2-T2 (Å)	3.776(5)	3.743(6)	3.715(6)	
T1-O45-T2 (°)	140.18(8)	136.48(9)	134.34(10)	
Φ (°)	17.15(8)	18.28(7)	20.03(9)	
ψ (°)	27.85(9)	26.73(8)	24.97(11)	
V Ba1 polyh. (Å^3)	49.99(4)	47.75(7)	46.99(8)	72(5)
Channel [001]				
O1 ↔ O1 (Å) ("free diameter")	1.989(7)	1.777(9)	1.515(9)	
O1 ↔ O1 (Å)	6.175(8)	6.211(7)	6.303(8)	
O23 ↔ O23 (Å)	0.839(6)	0.704(5)	0.706(7)	
O23-O1-O23 (°)	79.21(9)	76.65(8)	75.75(9)	
O45-O1-O45 (°)	108.74(10)	109.92(10	110.97(12)	
$\varepsilon_{[001]}$†	0.32	0.29	0.24	
$V_{ch\ 8\text{-}ring}$ (Å^3)	62.98(8)	56.08(8)	48.14(10)	19(1)
Channel [110]				
O1 ↔ O1 (Å)	3.834(6)	3.777(5)	3.727(6)	
O23 ↔ O23 (Å)	0.839(5)	0.704(5)	0.706(7)	
O45 ↔ O45 (Å)	2.750(7)	2.490(8)	2.261(8)	
O45 ↔ O45 (Å)	1.713(5)	1.659(5)	1.659(6)	
$\varepsilon_{[110]}$†	0.72	0.66	0.61	
$V_{ch\ 8\text{-}ring}$ (Å^3)	112.13(12)	98.80(18)	87.37(19)	21(1)

*Data collected under room conditions with the crystal in the DAC without a pressure medium.
† e.d.s. values are less than 0.005.

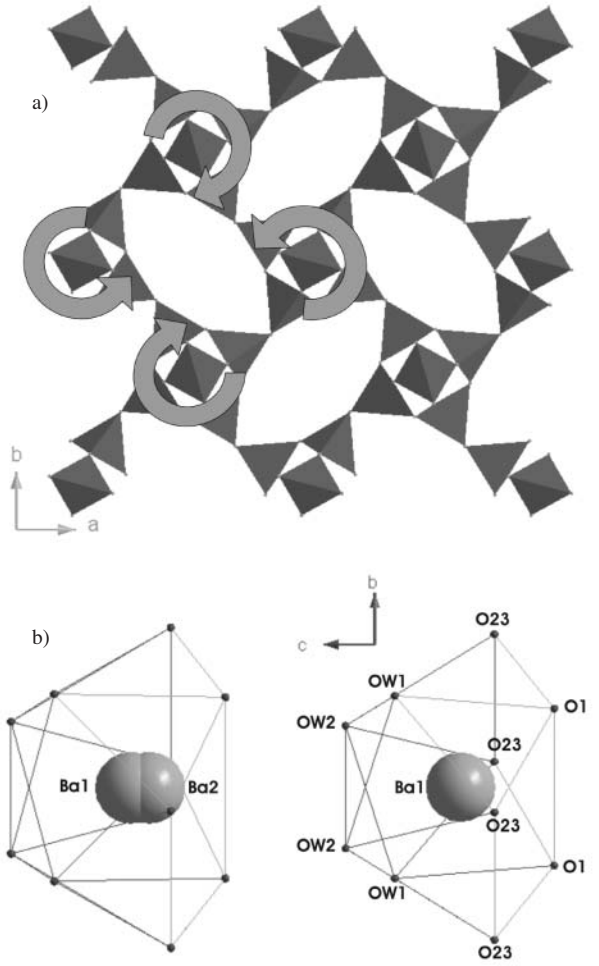

FIGURE 5. Structural effects due to increasing pressure: (**a**) SBU-antirotation mechanism; (**b**) topological modification of Ba polyhedron [0.0001 GPa on the left, 4.61(2) GPa on the right].

calculated from the free volume variations of the inscribed elliptical-section cylinders, are 19(1) and 21(1) GPa, respectively. Given the scarcity of data points, a linear regression between the data has been used to determine the compression coefficient of the channels and the coordination polyhedra.

Extra-framework cations and water molecules showed an interesting behavior under pressure conditions. The occupancy of the split Ba2 site decreased with pressure and, on the contrary, the occupancy coefficient for Ba1 site increased. At 4.61(2) GPa the Ba2 site is completely empty and only the position Ba1 is occupied (Table 3).

To analyze the effect of pressure on the extra-framework content the Ba-polyhedron volume was calculated at different pressures: 49.99(4) $Å^3$ at 0.0001 GPa, 47.75(7) $Å^3$ at 2.28(1) GPa, and 46.99(8)$Å^3$ at 4.61(2) GPa, with a bulk modulus of 72(4) GPa (Table 5). The e.s.d. for each volume value was calculated considering the larger and the smaller polyhedron volume due to the atomic position uncertainties.

Discussion

After scolecite and natrolite, edingtonite is the third fibrous zeolite studied at high pressures. Our high-pressure data show that the main deformation mechanism is represented by "anti-rotation" of the 4 = 1 SBU (Fig. 5); a similar mechanism was observed in scolecite by Comodi et al. (2002). The single SBU can be considered, as a first approximation, a relatively uncompressible "rigid unit". The rotation mechanism induces an axial compressibility that is smaller along [001] than [100]. Following the framework modifications, the free volumes of the two channel systems are strongly reduced with increasing pressure: the bulk moduli of both channels are about 20 GPa. We can conclude that the edingtonite bulk compression results from the combination of the soft behavior of the not fully occupied channels and of the rigid behavior of the tetrahedral framework.

As observed, the occupancy of the split Ba2 site decreases with pressure and it is completely empty at 4.61(2) GPa (Table 3). According to Mazzi et al. (1984) the split and poorly occupied Ba2 site, not observed in previous studies of orthorhombic edingtonite (Galli 1976; Kvick and Smith 1983), arises from the not fully occupied water molecule sites and the anomalous set of distances between the Ba1 site and framework/water molecules O atoms, which form the Ba-coordination sphere. In fact, the distances between Ba1-framework O atoms are longer than the distances between Ba1-water molecules (Table 4), a configuration that is the opposite of that normally found in zeolites. We can assume that the occupancy for the water sites does not change with increasing pressure, but the Ba1-OW1 and Ba1-OW2 distances decrease by about 2.1%, whereas the Ba1-O1 and Ba1-O23 distances are reduced by 5.8% and 1.6%, respectively (Table 4), in response to an applied pressure of 4.61(2) GPa. The high uncertainty of the Ba2-O bond distances, due to the extremely low occupancy of this site, does not allow analysis of this set of distances under H*P* conditions. The sensible volume reduction of the Ba polyhedron [49.99(4) $Å^3$ at 0.0001 GPa, 47.75(7) $Å^3$ at 2.28(1) GPa, Table 5] gives rise to an H*P*-topological configuration that is energetically favorable for the Ba1 site, which may explain why only one Ba-site is found in the structural refinements.

The structural modifications induced in edingtonite by an applied pressure are less dramatic than the effects observed at high temperature. Ståhl and Hanson (1998) showed a continuous loss of water, with increasing temperature, up to 660 K. The same chain rotations are observed as a response to an increase in temperature, because the loss of water molecules reduces the free volume of the channels. An unstable Ba-O coordination at $T >$ 660 K, due to the dehydration process, induces a rapid collapse of the crystal structure between 660 and 680 K.

In our study, the crystal structure is preserved at least up to 5.5 GPa and the structural modifications are completely reversible, as showed by the fact that lattice parameters collected with increasing pressure are indistinguishable from those collected during decompression (Fig. 1, Table 2)

Acknowledgments

Thanks are due to E. Galli and E. Passaglia for the sample of edingtonite from Ice River and for the chemical analysis. A special thank is due to S. Zanardi for determination of the Al-content of the tetrahedra. This work was financially supported by a Sofia Kovalevskaja Award to T. Boffa Ballaran and by Italian C.N.R and M.U.R.S.T grant to P.F. Zanazzi.

References cited

Alberti, A. and Gottardi, G. (1988) The determination of Al-content in the tetrahedra of framework silicates. Zeitschrift für Kristallographie, 184, 49-61.

Alberti, A. and Vezzalini, G. (1981) A partially disordered natrolite: relationships between cell parameters and Si-Al distribution. Acta Crystallographica, B37, 781–788.

Allan, D.R., Miletich, R., and Angel, R.J. (1996) A diamond-anvil cell for single-crystal X-ray diffraction studies to pressures in excess of 10 GPa. Review of Scientific Instruments, 67, 840–842.

Angel, R.J. (2000) Equation of state. In R.M. Hazen and R.T. Downs, Eds., High-Temperature and High-Pressure Crystal Chemistry, 41, 35–59. Reviews in Mineralogy and Geochemistry, Mineralogical Society of America and the Geochemical Society, Washington, D.C.

——— (2001) EOS-FIT V6.0. Computer program. Crystallography Laboratory, Department of Geological Sciences, Virginia Tech, Blacksburg, U.S.A.

——— (2002) ABSORB V5.2. Computer program. Crystallography Laboratory, Department of Geological Sciences, Virginia Tech, Blacksburg, U.S.A.

——— (2003a) Automated profile analysis for single-crystal diffraction data. Journal of Applied Crystallography, 36, 295–300.

——— (2003b) WIN-INTEGRSTP V3.4. Computer program. Crystallography Laboratory, Department of Geological Sciences, Virginia Tech, Blacksburg, U.S.A.

Angel, R.J., Allan, D.R., Miletich, R., and Finger, L.W. (1997) The use of quartz as an internal pressure standard in high-pressure crystallography. Journal of Applied Crystallography, 30, 461–466.

Angel, R.J., Downs, R.T., and Finger, L.W. (2000) High-temperature-high-pressure diffractometry. In R.M. Hazen and R.T. Downs, Eds., High-Temperature and High-Pressure Crystal Chemistry. Reviews in Mineralogy and Geochemistry, 41, 559–596. The Mineralogical Society of America and the Geochemical Society, Washington, D.C.

Armbruster, T. and Gunter, M.E. (2001) Crystal structures of natural zeolites. In D.L. Bish and D.W. Ming, Eds., Natural zeolites: Occurrence, properties, application. Review in Mineralogy and Geochemistry, 45, 1–57. The Mineralogical Society of America and the Geochemical Society, Washington, D.C.

Baerlocher, Ch., Meier, W.M., and Olson, D.H. (2001) Atlas of Zeolite Framework Types, 5th ed., 302 p. Elsevier, Amsterdam, Netherlands.

Ballone, P., Quartieri, S., Sani, A., and Vezzalini, G. (2002) High-pressure deformation mechanism in scolecite: A combined computational-experimental study. American Mineralogist, 87, 1194–1206.

Baur, W.H., Kassner, D., Kim, C.H., and Sieber, N.H.W. (1990) Flexibility and distortion of the framework of natrolite: crystal structures of ion-exchanged natrolites. European Journal of Mineralogy, 2, 761–769.

Belitsky, I.A., Gabuda, S.P., Joswig, W., and Fuess, H. (1986) Study of the structure and dynamics of water in the zeolite edingtonite at low temperature by neutron diffraction and NMR-spectroscopy. Neues Jahrbuch für Mineralogie Monatshefte, 1986(H12), 541–551.

Belitsky, I.A., Fursenko, B.A., Gabuda, S.P., Kholdeev, O.V., and Seryotkin, Y.V. (1992) Structural transformation in natrolite and edingtonite. Physics and Chemistry of Minerals, 18, 497–505.

Birch, F. (1947) Finite elastic strain of cubic crystal. Physical Review, 71, 809–824.

Burnham, C.W. (1966) Computation of absorption corrections and the significance of end effects. American Mineralogist, 51, 159–167.
Comodi, P., Gatta, G.D., and Zanazzi, P.F. (2001) High-pressure structural behavior of heulandite. European Journal of Mineralogy, 13, 497–505.
——— (2002) High-pressure behavior of scolecite. European Journal of Mineralogy, 14, 567–574.
——— (2003) Effects of pressure on the structure of bikitaite. European Journal of Mineralogy, 15, 247–225.
Galli, E. (1976) Crystal structure refinement of edingtonite. Acta Crystallographica, B32, 1623–1627.
Gatta, G.D., Comodi, P., and Zanazzi, P.F. (2003) New insights on high-pressure behavior of microporous materials from X-ray single-crystal data. Microporous and Mesoporous Materials, 61, 105–115.
Goryainov, S.V. and Belitsky, I.A. (1986) Analysis of vibrational spectra and phase transitions in zeolite (natrolite, edingtonite, chabasite). Proceedings of the Second International Conference on "Occurrence, Properties and Utilization of Natural Zeolites," 257–264, Budapest, Hungary.
Goryainov, S.V. and Smirnov, M.B. (2001) Raman spectra and lattice-dynamical calculations of natrolite. European Journal of Mineralogy, 13, 507–519.
Gottardi, G. and Galli, E. (1985) Natural Zeolites, 409 p. Springer-Verlag, Berlin.
Hazen, R.M. and Finger, L.W. (1979) Polyhedral tilting: a common type of pure displacive phase transition and its relationship to analcite at high pressure. Phase Transitions, 1, 1–22.
——— (1984) Compressibility of zeolite 4A is dependent on the molecular size of the hydrostatic pressure medium. Journal of Applied Physics, 56, 1838–1840.
Heinz, D.L. and Jeanloz, R. (1984) The equation of state of the gold calibration standard. Journal of Applied Physics, 55, 885–893.
Ibers, J.A. and Hamilton, W.C., Eds. (1974) International Tables for X-ray Crystallography, vol. IV, Kynoch, Birmingham, U.K.
Jones, J.B. (1968) Al-O and Si-O tetrahedral distances in aluminosilicate framework structures. Acta Crystallographica, B24, 355–358.
King, H.E. and Finger, L.W. (1979) Diffracted beam crystal centering and its application to high-pressure crystallography. Journal of Applied Crystallography, 12, 374–378.
Kvick, A. and Smith, J.V. (1983) A neutron diffraction study of the zeolite edingtonite. Journal of Chemical Physics, 79, 2356–2362.
Lee, Y., Vogt, T., Hriljac, J.A., Parise, J.B., and Artioli, A. (2002) Pressure-Induced Volume Expansion of Zeolites in the Natrolite Family. Journal of the American Chemical Society, 124, 5466–5475.
Mao, H.K., Xu, J., and Bell, P.M. (1986) Calibration of the ruby pressure gauge to 800 kbar under quasi-hydrostatic conditions. Journal of Geophysical Research, 91, 4673–4676.
Mazzi, F., Galli, E., and Gottardi, G. (1984) Crystal structure refinement of two tetragonal edingtonites. Neues Jahrbuch für Mineralogie Monatshefte, 1984(H8), 373–382.
Sheldrick, G.M. (1996) SADABS. Program for empirical absorption correction of area detector data. Institut für Anorganische Chemie, Universität Göttingen.
——— (1997) SHELX-97. Programs for crystal structure determination and refinement. Institut für Anorganische Chemie, Universität Göttingen, Germany.
Ståhl, K. and Hanson, J.C. (1998) An in situ study of the edingtonite dehydration process from X-ray synchrotron powder diffraction. European Journal of Mineralogy, 10, 221–228.
Taylor, W.H. and Jackson, R. (1933) The structure of edingtonite. Zeitschrift für Kristallographie, 86, 53–64.
Van Reeuwijk, L.P. (1972) High temperature phases of zeolites of the natrolite group. American Mineralogist, 57, 499–510.
——— (1974) The thermal dehydration of natural zeolites. PhD Thesis–Dissertation n. 587, 88 p., Wageningen Universiteit, Netherlands.

MANUSCRIPT RECEIVED JUNE 30, 2003
MANUSCRIPT ACCEPTED OCTOBER 19, 2003
MANUSCRIPT HANDLED BY THOMAS DUFFY